Radar-based Tree Detection and Mapping for Autonomous Navigation in Fruit Orchards

UC Chile SmartFarm Radar Team

School of Engineering
Pontificia Universidad Católica de Chile

IEEE AESS Radar Challenge
– 2025 –

Robotics and Automation Laboratory
Departamento de Ingeniería Eléctrica
Pontificia Universidad Católica De Chile

Tree Detection and Mapping for Autonomous Navigation in Fruit Orchards - IEEE AESS Radar Challenge 2025

Research Team

- Diego Muñoz Rojas
- Octavio Aguila-Rigordi
- Paola Nazate-Burgos

Project Advisor:

- Prof. Miguel Torres-Torriti

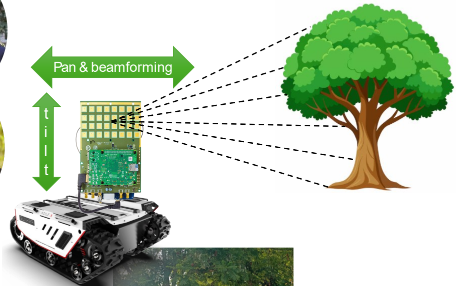

Project Summary

To develop a 3D perception system for 2D mapping of agricultural environments, using Frequency Modulated Continuous Wave (FMCW) processing and Constant False Alarm Rate (CFAR) detection techniques, and integrating Synthetic Aperture Radar (SAR), beamforming, and Simultaneous Localization and Mapping (SLAM), in order to implement algorithms capable of generating images that allow the identification of trees in fruit orchards.

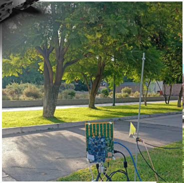

ral.ing.puc.cl

Robotics & Automation Laboratory
School of Engineering
PONTIFICIA UNIVERSIDAD CATÓLICA DE CHILE

ROS2 Integration

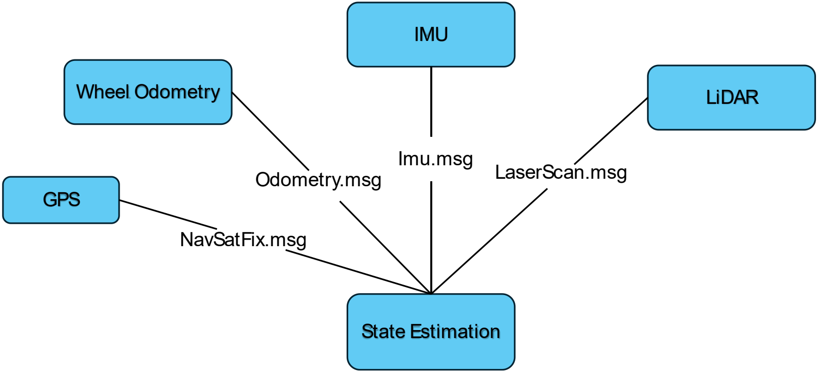

ROS2 Integration

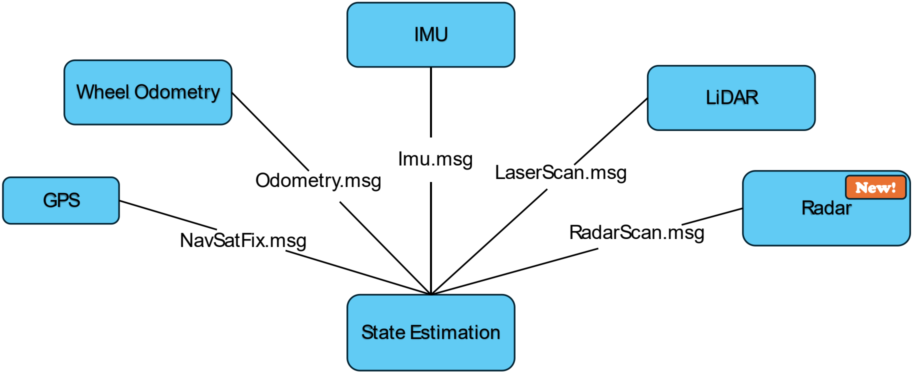

Sturcture of the Radar Message

ROS2 Integration: RadarData.msg

GitHub
https://github.com/RAL-UC/UC_SmartFarmRadar

```
std_msgs/Header header

# Dimensions
uint32 rows
uint32 cols
string dtype

# Radar data
float64[] data_real
float64[] data_imag

# Pan and tilt of the radar sensor in degrees
int32 pan_deg
int32 tilt_deg

# Robot pose
uint32 robot_pose_id
```

System Architecture

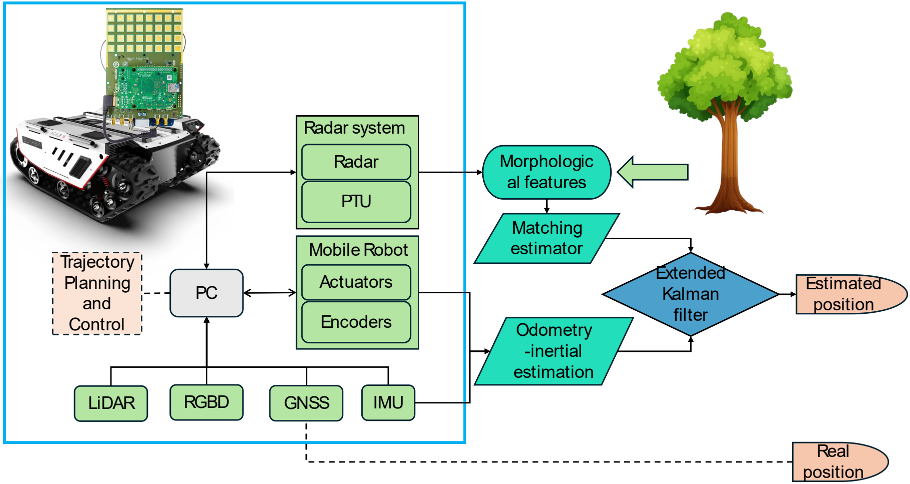

Overview SLAM

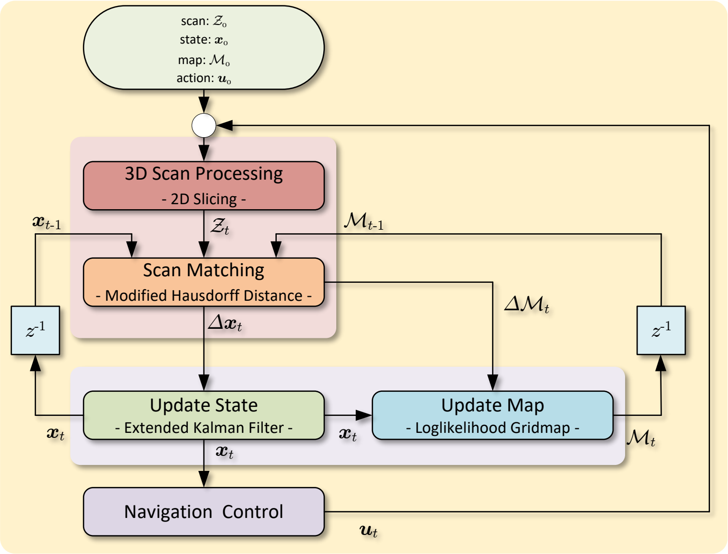

Objectives

1. Apply beamforming and SAR techniques using a pan-tilt unit (PTU) integrated into the mobile platform to obtain radar images of the agricultural environment.
2. Implement FMCW signal processing to interpret data and detect both vegetation and obstacles.
3. Develop algorithms for the identification, recognition, and classification of vegetation and obstacles, enabling the autonomous platform to effectively respond to their presence.
4. Implement a SLAM system to provide platform localization and a consistent map of the agricultural environment.
5. Evaluate the system's ability to generate useful information for optimizing and planning routes in an autonomous navigation system.
6. Create an application protocol and best practices to guide future agricultural research based on phased-array radars, establishing transferable knowledge for subsequent studies and developments in the field.

Objectives

1. Apply beamforming and SAR techniques using a pan-tilt unit (PTU) integrated into the mobile platform to obtain radar images of the agricultural environment.
2. Implement FMCW signal processing to interpret data and detect both vegetation and obstacles.
3. Develop algorithms for the identification, recognition, and classification of vegetation and obstacles, enabling the autonomous platform to effectively respond to their presence.
4. Implement a SLAM system to provide platform localization and a consistent map of the agricultural environment.
5. Evaluate the system's ability to generate useful information for optimizing and planning routes in an autonomous navigation system.
6. Create an application protocol and best practices to guide future agricultural research based on phased-array radars, establishing transferable knowledge for subsequent studies and developments in the field.

Objectives

1. Apply beamforming and SAR techniques using a pan-tilt unit (PTU) integrated into the mobile platform to obtain radar images of the agricultural environment.
2. Implement FMCW signal processing to interpret data and detect both vegetation and obstacles.
3. Develop algorithms for the identification, recognition, and classification of vegetation and obstacles, enabling the autonomous platform to effectively respond to their presence.
4. Implement a SLAM system to provide platform localization and a consistent map of the agricultural environment.
5. Evaluate the system's ability to generate useful information for optimizing and planning routes in an autonomous navigation system.
6. Create an application protocol and best practices to guide future agricultural research based on phased-array radars, establishing transferable knowledge for subsequent studies and developments in the field.

Objectives

1. Apply beamforming and SAR techniques using a pan-tilt unit (PTU) integrated into the mobile platform to obtain radar images of the agricultural environment.
2. Implement FMCW signal processing to interpret data and detect both vegetation and obstacles.
3. Develop algorithms for the identification, recognition, and classification of vegetation and obstacles, enabling the autonomous platform to effectively respond to their presence.
4. Implement a SLAM system to provide platform localization and a consistent map of the agricultural environment.
5. Evaluate the system's ability to generate useful information for optimizing and planning routes in an autonomous navigation system.
6. Create an application protocol and best practices to guide future agricultural research based on phased-array radars, establishing transferable knowledge for subsequent studies and developments in the field.

Objectives

1. Apply beamforming and SAR techniques using a pan-tilt unit (PTU) integrated into the mobile platform to obtain radar images of the agricultural environment.
2. Implement FMCW signal processing to interpret data and detect both vegetation and obstacles.
3. Develop algorithms for the identification, recognition, and classification of vegetation and obstacles, enabling the autonomous platform to effectively respond to their presence.
4. Implement a SLAM system to provide platform localization and a consistent map of the agricultural environment.
5. Evaluate the system's ability to generate useful information for optimizing and planning routes in an autonomous navigation system.
6. Create an application protocol and best practices to guide future agricultural research based on phased-array radars, establishing transferable knowledge for subsequent studies and developments in the field.

Objectives

1. Apply beamforming and SAR techniques using a pan-tilt unit (PTU) integrated into the mobile platform to obtain radar images of the agricultural environment.
2. Implement FMCW signal processing to interpret data and detect both vegetation and obstacles.
3. Develop algorithms for the identification, recognition, and classification of vegetation and obstacles, enabling the autonomous platform to effectively respond to their presence.
4. Implement a SLAM system to provide platform localization and a consistent map of the agricultural environment.
5. Evaluate the system's ability to generate useful information for optimizing and planning routes in an autonomous navigation system.
6. Create an application protocol and best practices to guide future agricultural research based on phased-array radars, establishing transferable knowledge for subsequent studies and developments in the field.

Contributions

1. A ROS 2-based architecture was implemented to enable electronic control of the radar using beamforming techniques.
2. Data acquisition routines were developed for the implementation of the SAR technique, providing the radar with two degrees of freedom through the PTU.
3. The fusion of dual radar-PTU sweeps was implemented into the SAR processing flow, generating environmental maps of the agricultural surroundings.
4. A predefined navigation trajectory was programmed for the mobile platform to acquire different maps oriented toward SLAM applications.
5. A multimodal navigation dataset was created by integrating information from sensors such as camera, LiDAR, GNSS, IMU, encoders, and radar, along with the commands sent to the actuators.

Contributions

1. A ROS 2-based architecture was implemented to enable electronic control of the radar using beamforming techniques.
2. Data acquisition routines were developed for the implementation of the SAR technique, providing the radar with two degrees of freedom through the PTU.
3. The fusion of dual radar-PTU sweeps was implemented into the SAR processing flow, generating environmental maps of the agricultural surroundings.
4. A predefined navigation trajectory was programmed for the mobile platform to acquire different maps oriented toward SLAM applications.
5. A multimodal navigation dataset was created by integrating information from sensors such as camera, LiDAR, GNSS, IMU, encoders, and radar, along with the commands sent to the actuators.

Contributions

1. A ROS 2-based architecture was implemented to enable electronic control of the radar using beamforming techniques.
2. Data acquisition routines were developed for the implementation of the SAR technique, providing the radar with two degrees of freedom through the PTU.
3. The fusion of dual radar-PTU sweeps was implemented into the SAR processing flow, generating environmental maps of the agricultural surroundings.
4. A predefined navigation trajectory was programmed for the mobile platform to acquire different maps oriented toward SLAM applications.
5. A multimodal navigation dataset was created by integrating information from sensors such as camera, LiDAR, GNSS, IMU, encoders, and radar, along with the commands sent to the actuators.

Contributions

1. A ROS 2-based architecture was implemented to enable electronic control of the radar using beamforming techniques.
2. Data acquisition routines were developed for the implementation of the SAR technique, providing the radar with two degrees of freedom through the PTU.
3. The fusion of dual radar-PTU sweeps was implemented into the SAR processing flow, generating environmental maps of the agricultural surroundings.
4. A predefined navigation trajectory was programmed for the mobile platform to acquire different maps oriented toward SLAM applications.
5. A multimodal navigation dataset was created by integrating information from sensors such as camera, LiDAR, GNSS, IMU, encoders, and radar, along with the commands sent to the actuators.

Contributions

1. A ROS 2-based architecture was implemented to enable electronic control of the radar using beamforming techniques.
2. Data acquisition routines were developed for the implementation of the SAR technique, providing the radar with two degrees of freedom through the PTU.
3. The fusion of dual radar-PTU sweeps was implemented into the SAR processing flow, generating environmental maps of the agricultural surroundings.
4. A predefined navigation trajectory was programmed for the mobile platform to acquire different maps oriented toward SLAM applications.
5. A multimodal navigation dataset was created by integrating information from sensors such as camera, LiDAR, GNSS, IMU, encoders, and radar, along with the commands sent to the actuators.

FMCW Radar: Preliminary notions, equations, and signal processing

$$
\begin{aligned}
\tau &= \frac{2r}{c} \\
f_m &= f_c + S\,\tau \\
f_b &= f_m - f_c = S\,\tau \\
r(f_m) &= \frac{(f_b - f_{bias})\,c}{2S} \\
S &= \frac{B}{T} \\
\Delta r &= \frac{c}{2B} = 0.3\ [m] \\
r_{\text{max tree}} &\approx 3.6\ [m]
\end{aligned}
$$

$$P_r = \frac{P_t G_t G_r \lambda^2 \sigma_s}{(4\pi)^3 r^4}$$

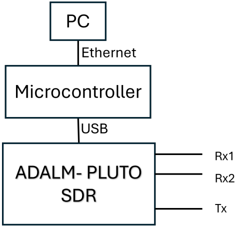

FMCW Radar: Preliminary notions, equations, and signal processing

$$
\begin{aligned}
\tau &= \frac{2r}{c} \\
f_m &= f_c + S\,\tau \\
f_b &= f_m - f_c = S\,\tau \\
r(f_m) &= \frac{(f_b - f_{bias})\,c}{2S} \\
S &= \frac{B}{T} \\
\Delta r &= \frac{c}{2B} = 0.3\ [m] \\
r_{\text{max tree}} &\approx 3.6\ [m]
\end{aligned}
$$

$$
P_r = \frac{P_t G_t G_r \lambda^2 \sigma_s}{(4\pi)^3 r^4}
$$

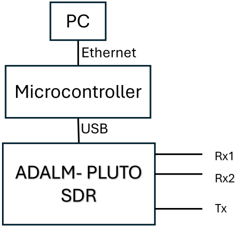

FMCW Radar: Preliminary notions, equations, and signal processing

$$\begin{aligned}
\tau &= \frac{2r}{c} \\
f_m &= f_c + S\,\tau \\
f_b &= f_m - f_c = S\,\tau \\
r(f_m) &= \frac{(f_b - f_{bias})\,c}{2S} \\
S &= \frac{B}{T} \\
\Delta r &= \frac{c}{2B} = 0.3\ [m] \\
r_{\text{max tree}} &\approx 3.6\ [m]
\end{aligned}$$

$$P_r = \frac{P_t G_t G_r \lambda^2 \sigma_s}{(4\pi)^3 r^4}$$

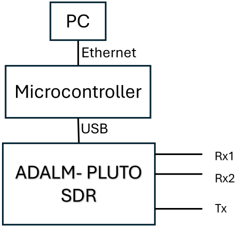

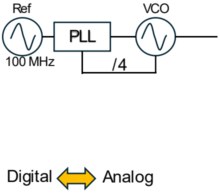

FMCW Radar: Preliminary notions, equations, and signal processing

$$
\begin{aligned}
\tau &= \frac{2r}{c} \\
f_m &= f_c + S\,\tau \\
f_b &= f_m - f_c = S\,\tau \\
r(f_m) &= \frac{(f_b - f_{bias})\,c}{2S} \\
S &= \frac{B}{T} \\
\Delta r &= \frac{c}{2B} = 0.3\ [m] \\
r_{\text{max tree}} &\approx 3.6\ [m]
\end{aligned}
$$

$$
P_r = \frac{P_t G_t G_r \lambda^2 \sigma_s}{(4\pi)^3 r^4}
$$

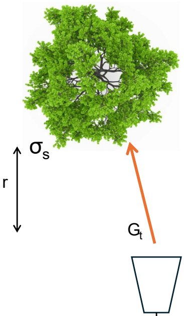

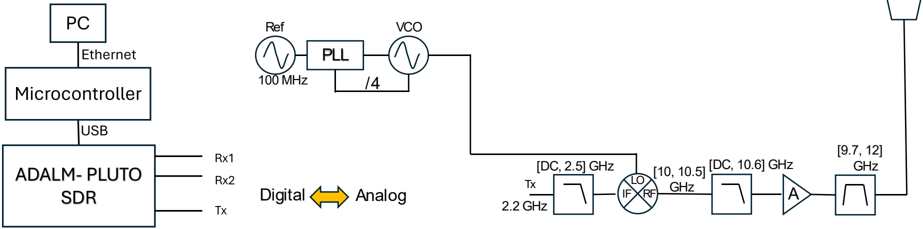

FMCW Radar: Preliminary notions, equations, and signal processing

$$\begin{aligned}
\tau &= \frac{2r}{c} \\
f_m &= f_c + S\,\tau \\
f_b &= f_m - f_c = S\,\tau \\
r(f_m) &= \frac{(f_b - f_{bias})\,c}{2S} \\
S &= \frac{B}{T} \\
\Delta r &= \frac{c}{2B} = 0.3\ [m] \\
r_{\text{max tree}} &\approx 3.6\ [m]
\end{aligned}$$

$$P_r = \frac{P_t G_t G_r \lambda^2 \sigma_s}{(4\pi)^3 r^4}$$

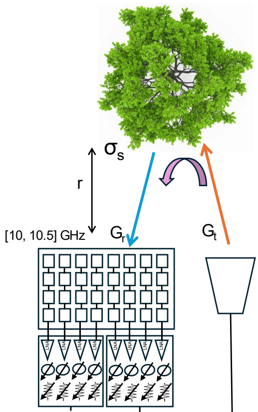

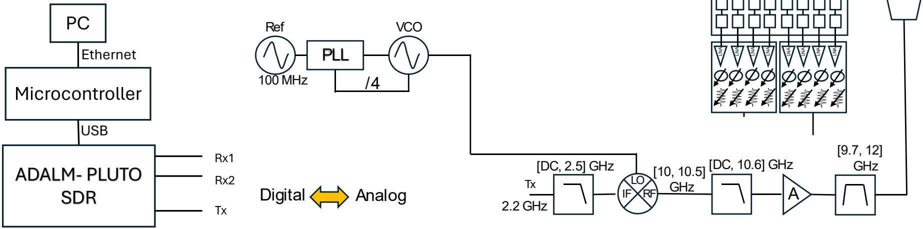

FMCW Radar: Preliminary notions, equations, and signal processing

$$
\begin{aligned}
\tau &= \frac{2r}{c} \\
f_m &= f_c + S\,\tau \\
f_b &= f_m - f_c = S\,\tau \\
r(f_m) &= \frac{(f_b - f_{bias})\,c}{2S} \\
S &= \frac{B}{T} \\
\Delta r &= \frac{c}{2B} = 0.3\ [m] \\
r_{\text{max tree}} &\approx 3.6\ [m]
\end{aligned}
$$

$$
P_r = \frac{P_t G_t G_r \lambda^2 \sigma_s}{(4\pi)^3 r^4}
$$

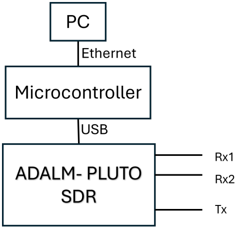

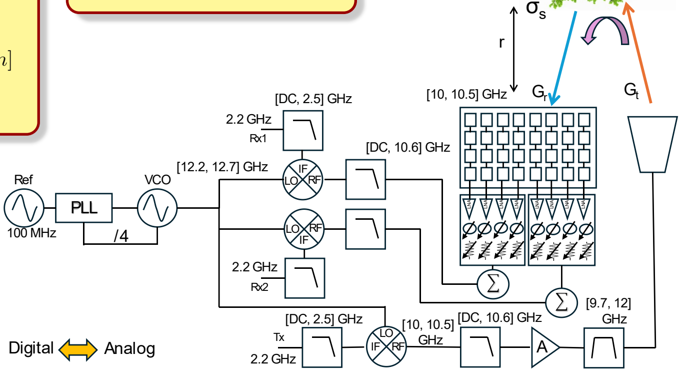

LFM Chirp Modulation and Averaging of Returns

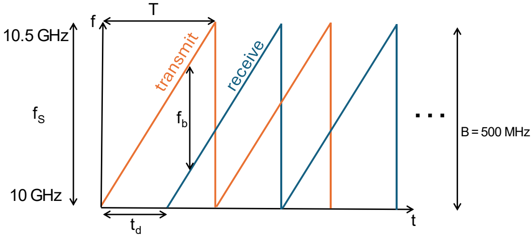

$$
\begin{aligned}
\phi(t) &= \pi S t^2 \\
f(t) &= \frac{1}{2\pi}\frac{d}{dt}\phi(t) \;=\; St \\
s_k(t) &= e^{j\phi(t)},\; 0 \le t \le T, \\
&\qquad\qquad k = 0, \ldots, M-1 \\
\bar{s}(t) &= \frac{1}{M}\sum_{k=0}^{M-1} s_k(t + kT)
\end{aligned}
$$

LFM Chirp Modulation and Averaging of Returns

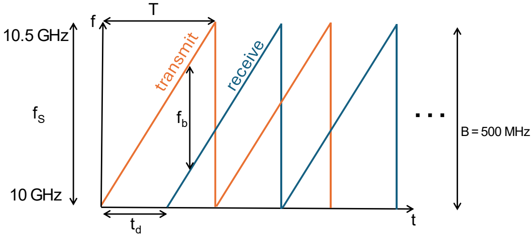

$$\begin{aligned}
\phi(t) &= \pi S t^2 \\
f(t) &= \frac{1}{2\pi}\frac{d}{dt}\phi(t) = St \\
s_k(t) &= e^{j\phi(t)},\ 0 \le t \le T, \\
&\qquad k = 0, \ldots, M-1 \\
\bar{s}(t) &= \frac{1}{M}\sum_{k=0}^{M-1} s_k(t + kT)
\end{aligned}$$

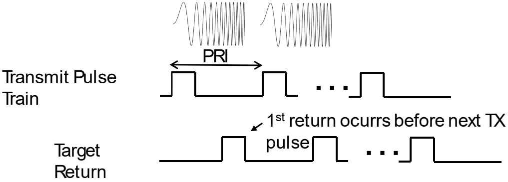

LFM Chirp Modulation and Averaging of Returns

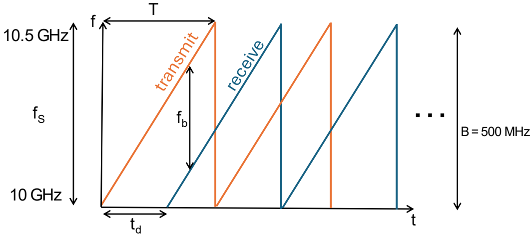

$$
\begin{aligned}
\phi(t) &= \pi S t^2 \\
f(t) &= \frac{1}{2\pi}\frac{d}{dt}\phi(t) = St \\
s_k(t) &= e^{j\phi(t)},\ 0 \le t \le T, \\
&\qquad k = 0, \ldots, M-1 \\
\bar{s}(t) &= \frac{1}{M}\sum_{k=0}^{M-1} s_k(t+kT)
\end{aligned}
$$

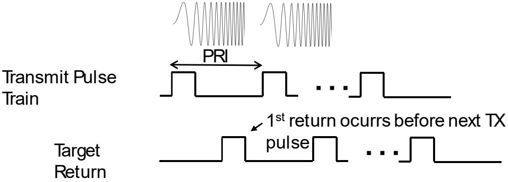

LFM Chirp Modulation and Averaging of Returns

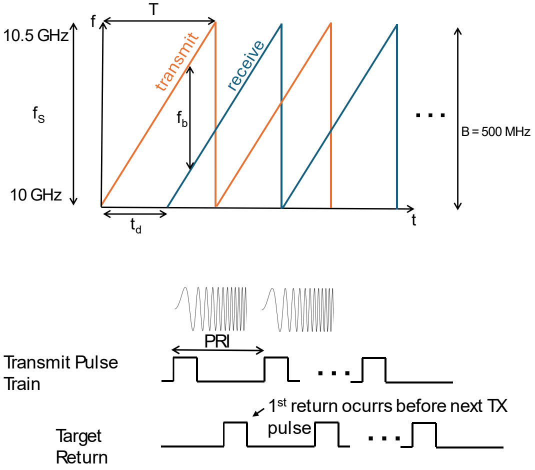

$$\phi(t) = \pi S t^2$$

$$f(t) = \frac{1}{2\pi}\frac{d}{dt}\phi(t) = St$$

$$s_k(t) = e^{j\phi(t)},\ 0 \le t \le T,$$
$$k = 0, \ldots, M-1$$

$$\bar{s}(t) = \frac{1}{M}\sum_{k=0}^{M-1} s_k(t + kT)$$

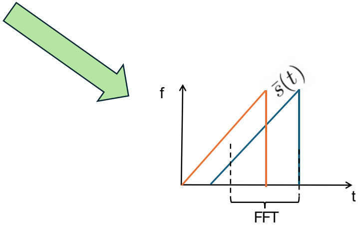

CFAR detections

Consider a radar measurement sequence:

$$S_k = \{X_1, X_2, \ldots, X_N\}, \qquad i \in \{N_g+N_r+1, \ldots, N-(N_g+N_r)\}$$

where X_i is the *intensity value* of the i-th cell, while N_g and N_r are the the number of so-called guard cells and reference cells.

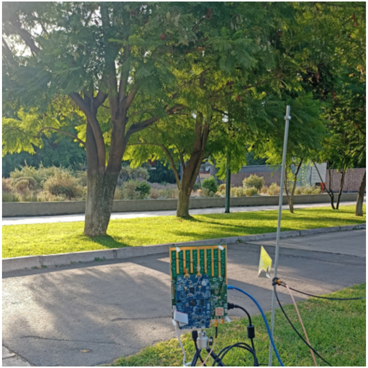

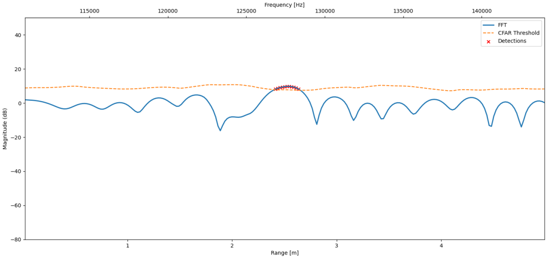

CFAR detections

The *lower, upper and full sets of reference cells* are defined as:

$$
\begin{aligned}
R_i^{low} &\stackrel{def}{=} \{X_{i-(N_g+N_r)},\ \ldots,\ X_{i-N_g-1}\}, \\
R_i^{up} &\stackrel{def}{=} \{X_{i+N_g+1}, \ldots, X_{i+(N_g+N_r)}\}, \\
R_i &\stackrel{def}{=} R_i^{low} \cup R_i^{up},
\end{aligned}
$$

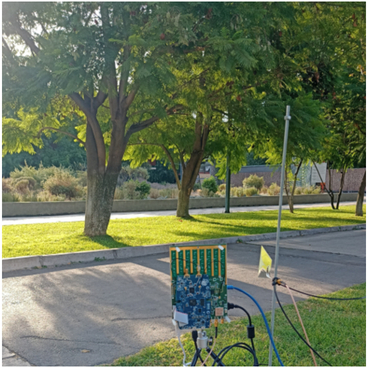

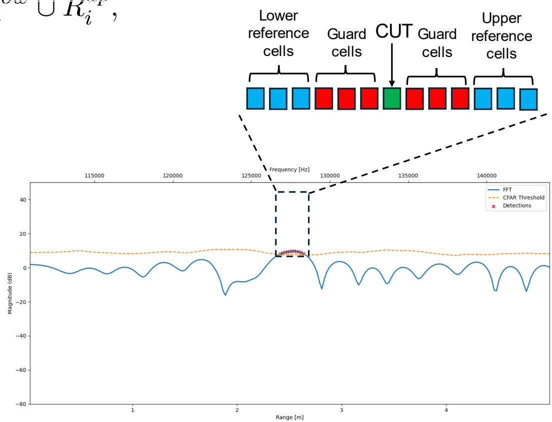

CFAR detections

The *adaptive threshold* at cell i with bias B is given by:

$$T_i \;=\; \frac{1}{2N_r}\sum_i R_i \;+\; B.$$

Finally, the *selection/rejection mask* is obtained as:

$$D \;=\; \{D_i | D_i = \mathbb{1}\,(X_i \geq T_i)\}$$

i.e. selecting all cells whose intensity $X_i \geq T_i$*.*

Phase Delay and Beam Formation

$$\Delta\phi^s(\theta^s) = \frac{2\pi\, f_{\mathsf{IF}}\, d\, \sin(\theta^s)}{c}$$

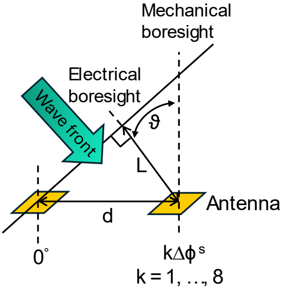

$$L = d\sin(\theta_s)$$

$$\Delta t = \frac{L}{c} = \frac{d\sin(\theta_s)}{c} \rightarrow \theta_s = \arcsin\left(\frac{\Delta t\, c}{d}\right)$$

$$\Delta\phi^s = \frac{2\pi L}{\lambda}$$

- $\Delta\phi^s(\theta^s)$ Incremental phase shift between elements.
- d Distance between the two antennas.
- θ^s Beam electrical angle.
- Δt Incremental time delay between elements.
- L Incremental propagation distance between elements
- f_{IF} Intermediate operating frequency

Phase Delay and Beam Formation

$$\Delta\phi^s(\theta^s) = \frac{2\pi\, f_{\mathrm{IF}}\, d\, \sin(\theta^s)}{c}$$

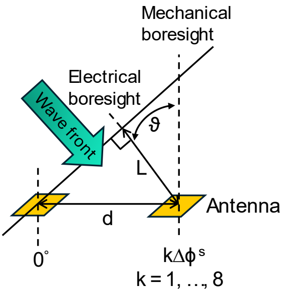

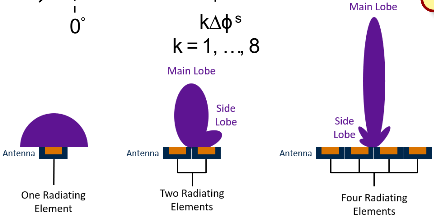

$$L = d\sin(\theta_s)$$

$$\Delta t = \frac{L}{c} = \frac{d\sin(\theta_s)}{c} \rightarrow \theta_s = \arcsin\left(\frac{\Delta t\, c}{d}\right)$$

$$\Delta\phi^s = \frac{2\pi L}{\lambda}$$

- $\Delta\phi^s(\theta^s)$ Incremental phase shift between elements.
- d Distance between the two antennas.
- θ^s Beam electrical angle.
- Δt Incremental time delay between elements.
- L Incremental propagation distance between elements
- f_{IF} Intermediate operating frequency

Phase Delay and Beam Formation

$$\Delta\phi^s(\theta^s) = \frac{2\pi\, f_{\mathsf{IF}}\, d\, \sin(\theta^s)}{c}$$

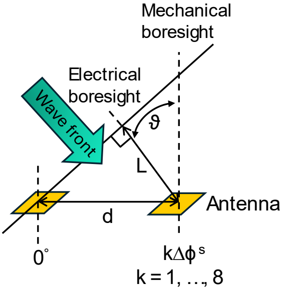

$$\begin{aligned} L &= d\sin(\theta_s) \\ \Delta t &= \frac{L}{c} = \frac{d\sin(\theta_s)}{c} \rightarrow \theta_s = \arcsin\left(\frac{\Delta t\, c}{d}\right) \\ \Delta\phi^s &= \frac{2\pi L}{\lambda} \end{aligned}$$

- $\Delta\phi^s(\theta^s)$ Incremental phase shift between elements.
- d Distance between the two antennas.
- θ^s Beam electrical angle.
- Δt Incremental time delay between elements.
- L Incremental propagation distance between elements
- f_{IF} Intermediate operating frequency

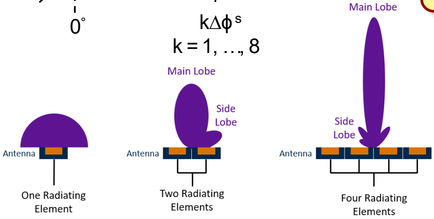

2D slice capture

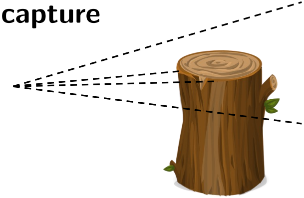

Navigation Equations

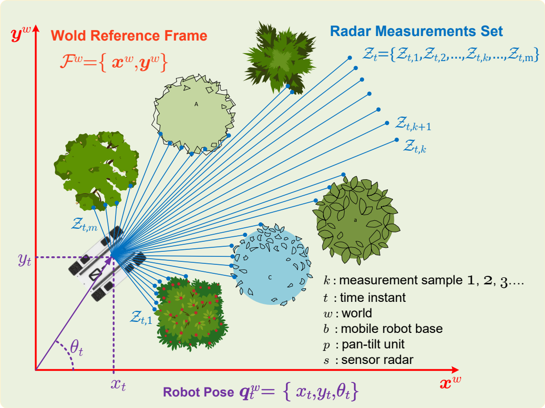

Navigation Equations

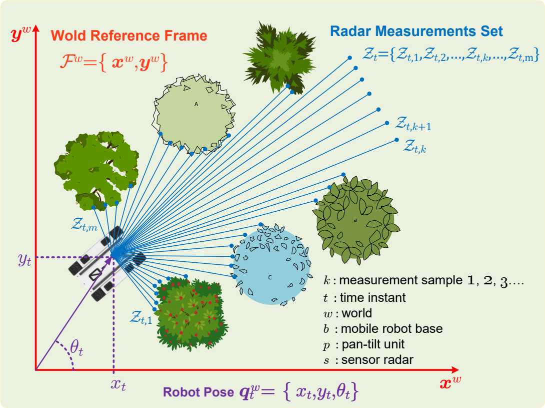

Radar measurement:

$$x^s = r \cos\theta^s, \quad y^s = r \sin\theta^s$$

Navigation Equations

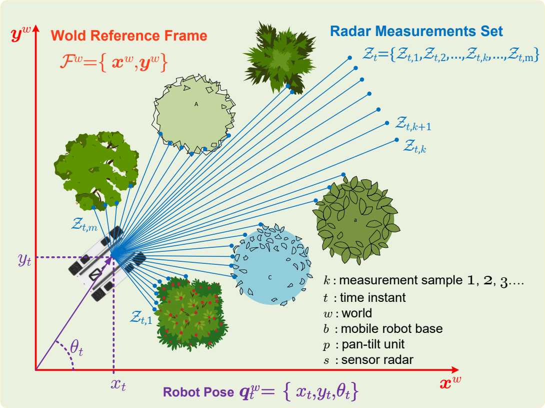

Radar measurement:

$$x^s = r\cos\theta^s, \quad y^s = r\sin\theta^s$$

Radar → Pan-Tilt:

$$\alpha^p = \theta^p + \theta^s, \qquad \rho = r\cos\phi^p$$

$$\begin{bmatrix} x^p \\ y^p \end{bmatrix} = \begin{bmatrix} \rho\cos\alpha^p \\ \rho\sin\alpha^p \end{bmatrix}$$

$$z^p = r\sin\phi^p \to 0$$

Navigation Equations

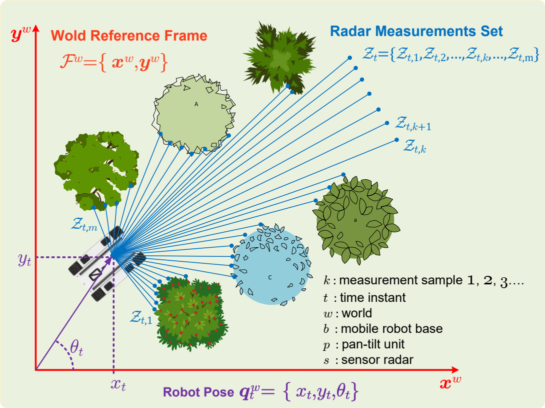

Radar measurement:

$$x^s = r\cos\theta^s, \quad y^s = r\sin\theta^s$$

Radar $\rightarrow$ Pan-Tilt:

$$\alpha^p = \theta^p + \theta^s, \qquad \rho = r\cos\phi^p$$

$$\begin{bmatrix} x^p \\ y^p \end{bmatrix} = \begin{bmatrix} \rho\cos\alpha^p \\ \rho\sin\alpha^p \end{bmatrix}$$

$$z^p = r\sin\phi^p \rightarrow 0$$

Pan-Tilt $\rightarrow$ Robot:

$$\begin{bmatrix} x^b \\ y^b \\ z^b \end{bmatrix} = \begin{bmatrix} x^p \\ y^p \\ z^p \end{bmatrix} + \begin{bmatrix} \ell_x \\ \ell_y \\ \ell_z \end{bmatrix}$$

Navigation Equations

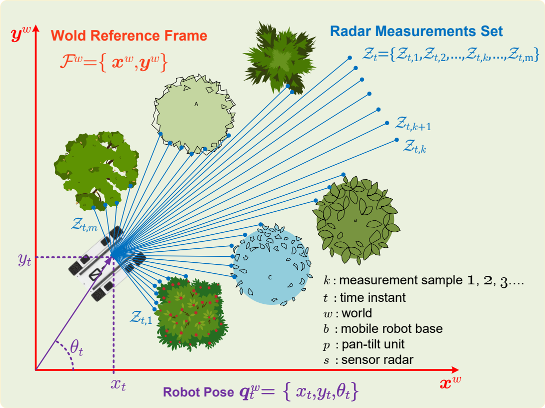

Radar measurement:

$$x^s = r \cos\theta^s, \quad y^s = r \sin\theta^s$$

Radar $\rightarrow$ Pan-Tilt:

$$\alpha^p = \theta^p + \theta^s, \qquad \rho = r\cos\phi^p$$

$$\begin{bmatrix} x^p \\ y^p \end{bmatrix} = \begin{bmatrix} \rho\cos\alpha^p \\ \rho\sin\alpha^p \end{bmatrix}$$

$$z^p = r\sin\phi^p \rightarrow 0$$

Pan-Tilt $\rightarrow$ Robot:

$$\begin{bmatrix} x^b \\ y^b \\ z^b \end{bmatrix} = \begin{bmatrix} x^p \\ y^p \\ z^p \end{bmatrix} + \begin{bmatrix} \ell_x \\ \ell_y \\ \ell_z \end{bmatrix}$$

Robot $\rightarrow$ World:

$$\begin{bmatrix} x^w \\ y^w \\ z^w \end{bmatrix} = \begin{bmatrix} x_b^w \\ y_b^w \\ z_b^w \end{bmatrix} + R_z(\theta^b) \begin{bmatrix} x^b \\ y^b \\ z^b \end{bmatrix}$$

Navigation Equations

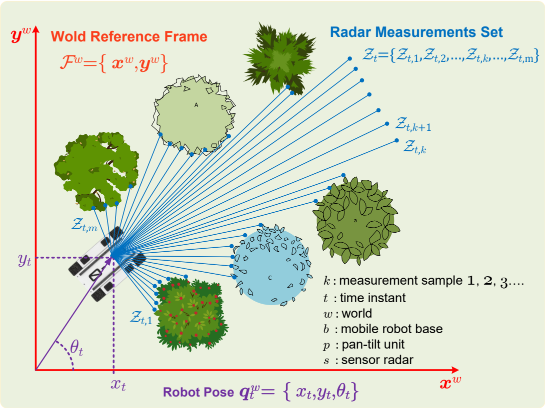

Sensor-to-World Coordinate Transformation: 2D projection map

$$
\begin{aligned}
x^w &= x_b^w + \ell_x \cos\theta^b - \ell_y \sin\theta^b + r\cos\phi^p \, \cos\left(\theta^p + \theta^s + \theta^b\right) \\
y^w &= y_b^w + \ell_x \sin\theta^b + \ell_y \cos\theta^b + r\cos\phi^p \, \sin\left(\theta^p + \theta^s + \theta^b\right) \\
z^w &= z_b^w + \ell_z
\end{aligned}
$$

Radar measurement:

$$
x^s = r\cos\theta^s, \quad y^s = r\sin\theta^s
$$

Radar $\rightarrow$ Pan-Tilt:

$$
\alpha^p = \theta^p + \theta^s, \qquad \rho = r\cos\phi^p
$$

$$
\begin{bmatrix} x^p \\ y^p \end{bmatrix} = \begin{bmatrix} \rho\cos\alpha^p \\ \rho\sin\alpha^p \end{bmatrix}
$$

$$
z^p = r\sin\phi^p \rightarrow 0
$$

Pan-Tilt $\rightarrow$ Robot:

$$
\begin{bmatrix} x^b \\ y^b \\ z^b \end{bmatrix} = \begin{bmatrix} x^p \\ y^p \\ z^p \end{bmatrix} + \begin{bmatrix} \ell_x \\ \ell_y \\ \ell_z \end{bmatrix}
$$

Robot $\rightarrow$ World:

$$
\begin{bmatrix} x^w \\ y^w \\ z^w \end{bmatrix} = \begin{bmatrix} x_b^w \\ y_b^w \\ z_b^w \end{bmatrix} + R_z(\theta^b) \begin{bmatrix} x^b \\ y^b \\ z^b \end{bmatrix}
$$

Dual-Sweep PTU-Radar Fusion in SAR Processing

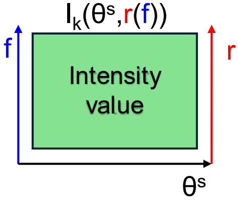

Dual-Sweep PTU-Radar Fusion in SAR Processing

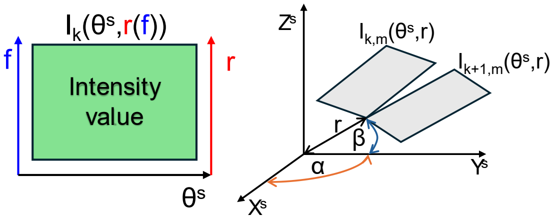

Dual-Sweep PTU-Radar Fusion in SAR Processing

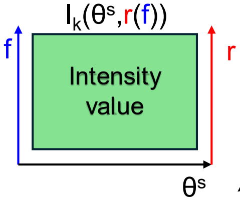

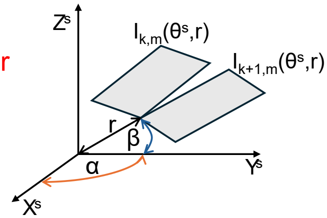

Angular range and resolution values:

$$\text{Azimuth: } \alpha \in [-170^\circ, 170^\circ]$$

$$\text{Elevation: } \beta \in [-20^\circ, 15^\circ]$$

$$\theta_n^s \in [-80^\circ, 80^\circ], \quad \theta_q^p \in [-90^\circ, 90^\circ]$$

$$\Delta\theta^p = 15^\circ, \quad \Delta\theta^s = 1^\circ, \quad \Delta\phi^p = 5^\circ$$

Dual-Sweep PTU-Radar Fusion in SAR Processing

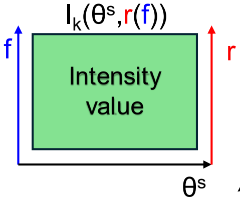

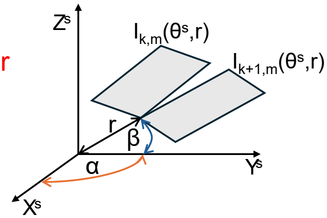

Angular range and resolution values:

Azimuth: $\alpha \in [-170°, 170°]$

Elevation: $\beta \in [-20°, 15°]$

$\theta_n^s \in [-80°, 80°], \quad \theta_q^p \in [-90°, 90°]$

$\Delta\theta^p = 15°, \quad \Delta\theta^s = 1°, \quad \Delta\phi^p = 5°$

Dual-Sweep PTU-Radar Fusion in SAR Processing

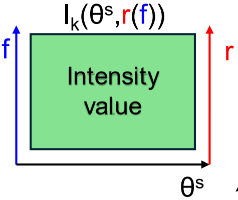

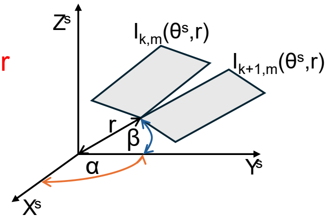

Angular range and resolution values:

Azimuth: $\alpha \in [-170°, 170°]$

Elevation: $\beta \in [-20°, 15°]$

$\theta_n^s \in [-80°, 80°], \quad \theta_q^p \in [-90°, 90°]$

$\Delta\theta^p = 15°, \quad \Delta\theta^s = 1°, \quad \Delta\phi^p = 5°$

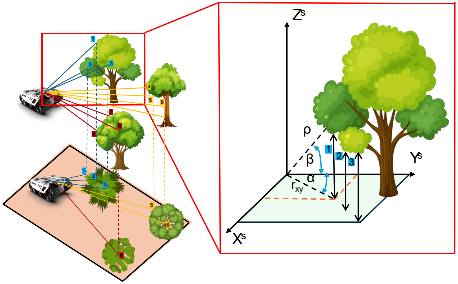

Dual-Sweep PTU-Radar Fusion in SAR Processing

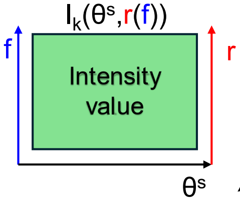

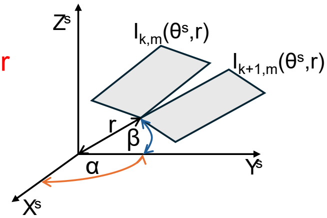

Angular range and resolution values:

Azimuth: $\alpha \in [-170°, 170°]$

Elevation: $\beta \in [-20°, 15°]$

$\theta_n^s \in [-80°, 80°], \quad \theta_q^p \in [-90°, 90°]$

$\Delta\theta^p = 15°, \quad \Delta\theta^s = 1°, \quad \Delta\phi^p = 5°$

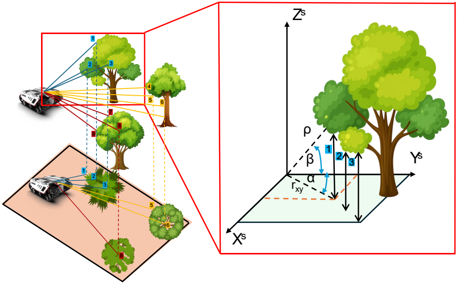

Dual-Sweep Angular Fusion: PTU+Radar

$$\alpha = \theta_q^p + \theta_n^s, \quad \beta = \phi_m^p$$

$$w_q(\alpha) = \max\left\{0,\ 1 - \frac{|\alpha - \theta_q^p|}{FOV/2}\right\}, \quad FOV = 160°$$

$$Q(\alpha) = \{q : |\alpha - \theta_q^p| \leq FOV/2\}$$

$$C(\alpha, \beta, r) = \frac{\sum_{q \in Q(\alpha)} w_q(\alpha)\ I_{q,m}\big(\Theta_q(\alpha), r\big)}{\sum_{q \in Q(\alpha)} w_q(\alpha)}$$

$$\rho = r\cos(\beta)$$

$$x^p = \rho\cos(\alpha), \quad y^p = \rho\sin(\alpha)$$

$$z^p = r\sin(\beta) \to 0$$

Background Noise Suppression

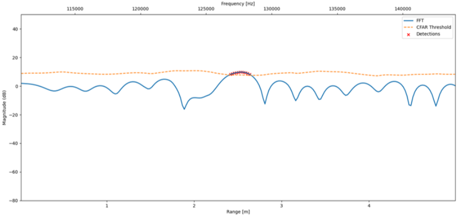

$$I^{bg}(\theta^s, f) = \frac{1}{N}\sum_{j=1}^{N} I_j^{bg}(\theta^s, f)$$
$$I(\theta^s, f) = I^{raw}(\theta^s, f) - I^{bg}(\theta^s, f)$$

Background Noise Suppression

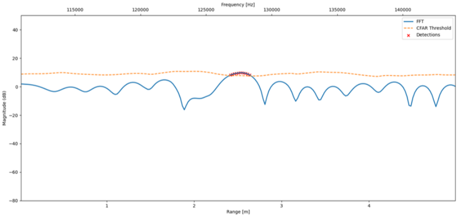

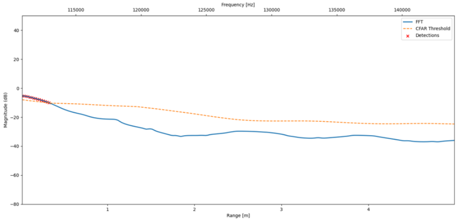

$$I^{bg}(\theta^s, f) = \frac{1}{N}\sum_{j=1}^{N} I_j^{bg}(\theta^s, f)$$
$$I(\theta^s, f) = I^{raw}(\theta^s, f) - I^{bg}(\theta^s, f)$$

Background Noise Suppression

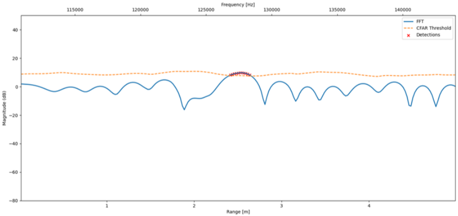

$$I^{bg}(\theta^s, f) = \frac{1}{N}\sum_{j=1}^{N} I_j^{bg}(\theta^s, f)$$
$$I(\theta^s, f) = I^{raw}(\theta^s, f) - I^{bg}(\theta^s, f)$$

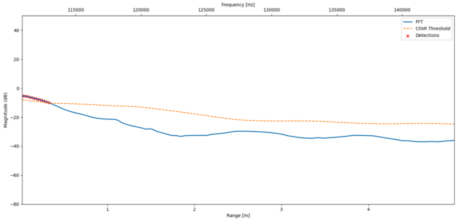

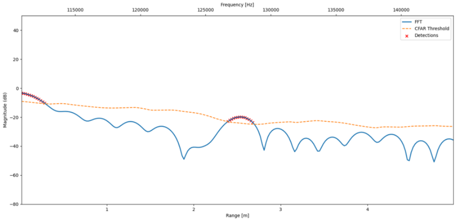

2D Map: Tree-facing Measurement

Tree at a distance of 2.4 meters

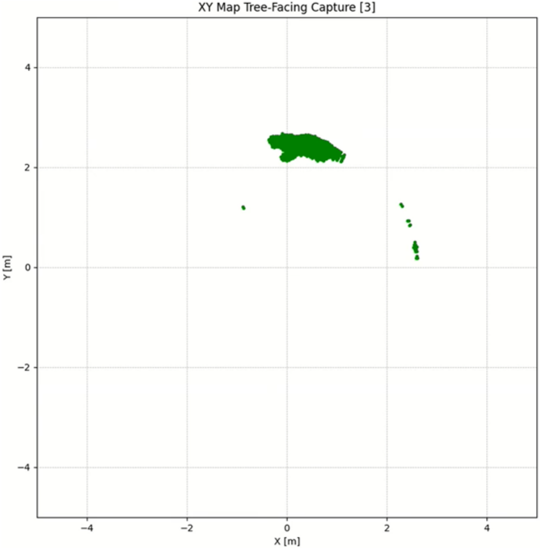

GitHub
https://github.com/RAL-UC/UC_SmartFarmRadar

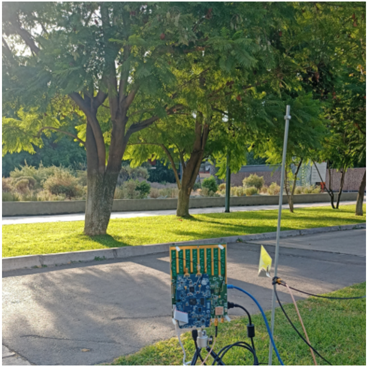

2D SLAM: Tree-facing Measurements

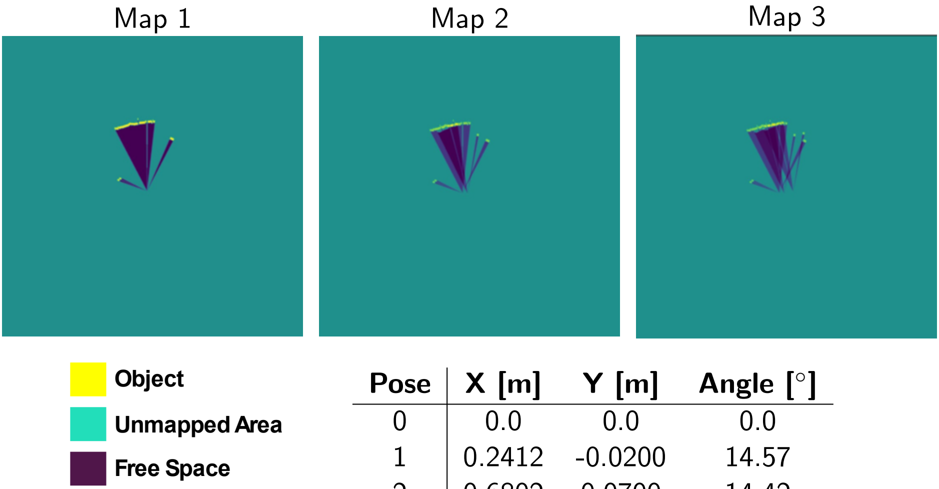

Pose	X [m]	Y [m]	Angle [°]
0	0.0	0.0	0.0
1	0.2412	-0.0200	14.57
2	0.6802	0.0700	14.42

2D SLAM: Estimated Trajectory

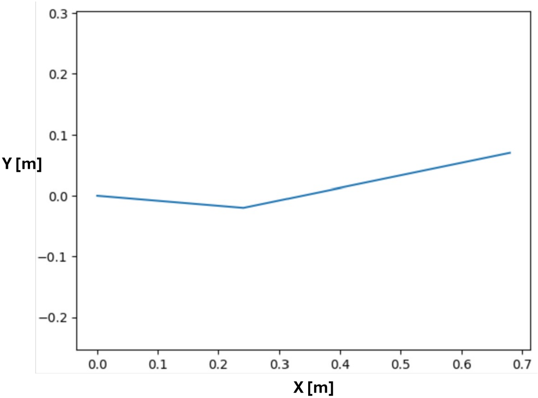

GitHub

https://github.com/RAL-UC/UC_SmartFarmRadar

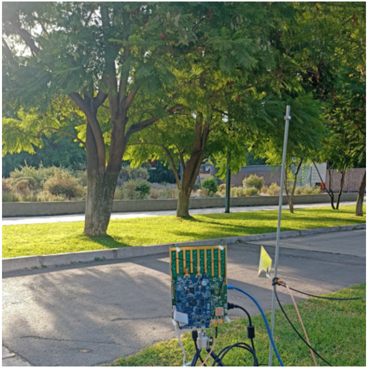

Future Work

- Simulation: PTU-radar package in Gazebo and wave simulator for algorithm validation.
- Modeling and compensation: incorporation of element and array characteristics to improve estimation accuracy.
- RCS characterization: estimation of vegetation radar cross-section under different conditions.
- Signal processing: integration of phase information for more precise estimation and application of MTI techniques for moving target detection and tracking.
- Sensor fusion: combination of radar, lidar an cameras to refine detection and vegetation pattern recognition.
- Artificial intelligence: development of machine learning-based classifiers to characterize vegetation and distinguish obstacles in agricultural environments.
- Protocol and best practices: Develop a usage protocol for application of phased-array radars in agricultural environments.

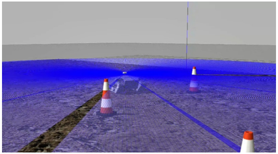

$$|s(t)| = \sqrt{I(t)^2 + Q(t)^2}$$
$$\angle s(t) = \arctan\left(\frac{Q(t)}{I(t)}\right)$$

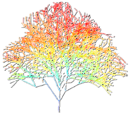

Future Work

- Simulation: PTU-radar package in Gazebo and wave simulator for algorithm validation.
- Modeling and compensation: incorporation of element and array characteristics to improve estimation accuracy.
- RCS characterization: estimation of vegetation radar cross-section under different conditions.
- Signal processing: integration of phase information for more precise estimation and application of MTI techniques for moving target detection and tracking.
- Sensor fusion: combination of radar, lidar an cameras to refine detection and vegetation pattern recognition.
- Artificial intelligence: development of machine learning-based classifiers to characterize vegetation and distinguish obstacles in agricultural environments.
- Protocol and best practices: Develop a usage protocol for application of phased-array radars in agricultural environments.

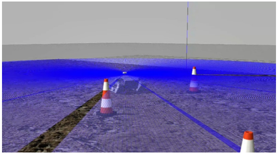

$$|s(t)| = \sqrt{I(t)^2 + Q(t)^2}$$
$$\angle s(t) = \arctan\left(\frac{Q(t)}{I(t)}\right)$$

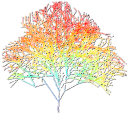

Future Work

- Simulation: PTU-radar package in Gazebo and wave simulator for algorithm validation.
- Modeling and compensation: incorporation of element and array characteristics to improve estimation accuracy.
- RCS characterization: estimation of vegetation radar cross-section under different conditions.
- Signal processing: integration of phase information for more precise estimation and application of MTI techniques for moving target detection and tracking.
- Sensor fusion: combination of radar, lidar an cameras to refine detection and vegetation pattern recognition.
- Artificial intelligence: development of machine learning-based classifiers to characterize vegetation and distinguish obstacles in agricultural environments.
- Protocol and best practices: Develop a usage protocol for application of phased-array radars in agricultural environments.

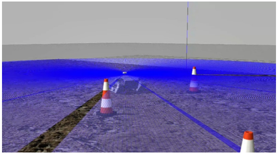

$$|s(t)| = \sqrt{I(t)^2 + Q(t)^2}$$
$$\angle s(t) = \arctan\left(\frac{Q(t)}{I(t)}\right)$$

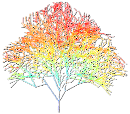

Future Work

- Simulation: PTU-radar package in Gazebo and wave simulator for algorithm validation.
- Modeling and compensation: incorporation of element and array characteristics to improve estimation accuracy.
- RCS characterization: estimation of vegetation radar cross-section under different conditions.
- Signal processing: integration of phase information for more precise estimation and application of MTI techniques for moving target detection and tracking.
- Sensor fusion: combination of radar, lidar an cameras to refine detection and vegetation pattern recognition.
- Artificial intelligence: development of machine learning-based classifiers to characterize vegetation and distinguish obstacles in agricultural environments.
- Protocol and best practices: Develop a usage protocol for application of phased-array radars in agricultural environments.

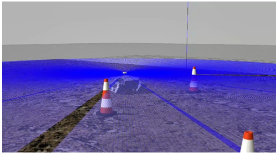

$$|s(t)| = \sqrt{I(t)^2 + Q(t)^2}$$
$$\angle s(t) = \arctan\left(\frac{Q(t)}{I(t)}\right)$$

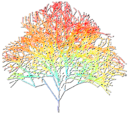

Future Work

- Simulation: PTU-radar package in Gazebo and wave simulator for algorithm validation.
- Modeling and compensation: incorporation of element and array characteristics to improve estimation accuracy.
- RCS characterization: estimation of vegetation radar cross-section under different conditions.
- Signal processing: integration of phase information for more precise estimation and application of MTI techniques for moving target detection and tracking.
- Sensor fusion: combination of radar, lidar an cameras to refine detection and vegetation pattern recognition.
- Artificial intelligence: development of machine learning-based classifiers to characterize vegetation and distinguish obstacles in agricultural environments.
- Protocol and best practices: Develop a usage protocol for application of phased-array radars in agricultural environments.

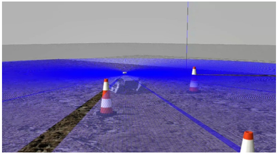

$$|s(t)| = \sqrt{I(t)^2 + Q(t)^2}$$
$$\angle s(t) = \arctan\left(\frac{Q(t)}{I(t)}\right)$$

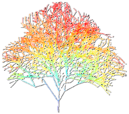

Future Work

- Simulation: PTU-radar package in Gazebo and wave simulator for algorithm validation.
- Modeling and compensation: incorporation of element and array characteristics to improve estimation accuracy.
- RCS characterization: estimation of vegetation radar cross-section under different conditions.
- Signal processing: integration of phase information for more precise estimation and application of MTI techniques for moving target detection and tracking.
- Sensor fusion: combination of radar, lidar an cameras to refine detection and vegetation pattern recognition.
- Artificial intelligence: development of machine learning-based classifiers to characterize vegetation and distinguish obstacles in agricultural environments.
- Protocol and best practices: Develop a usage protocol for application of phased-array radars in agricultural environments.

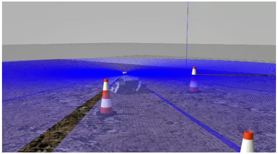

$$|s(t)| = \sqrt{I(t)^2 + Q(t)^2}$$
$$\angle s(t) = \arctan\left(\frac{Q(t)}{I(t)}\right)$$

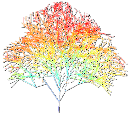

Future Work

- Simulation: PTU-radar package in Gazebo and wave simulator for algorithm validation.
- Modeling and compensation: incorporation of element and array characteristics to improve estimation accuracy.
- RCS characterization: estimation of vegetation radar cross-section under different conditions.
- Signal processing: integration of phase information for more precise estimation and application of MTI techniques for moving target detection and tracking.
- Sensor fusion: combination of radar, lidar an cameras to refine detection and vegetation pattern recognition.
- Artificial intelligence: development of machine learning-based classifiers to characterize vegetation and distinguish obstacles in agricultural environments.
- Protocol and best practices: Develop a usage protocol for application of phased-array radars in agricultural environments.

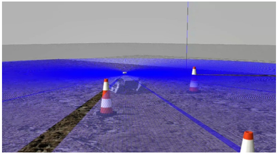

$$|s(t)| = \sqrt{I(t)^2 + Q(t)^2}$$
$$\angle s(t) = \arctan\left(\frac{Q(t)}{I(t)}\right)$$

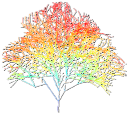

Acknowledgements

Huge thanks to...

The organizers of the Radar Challenge 2025 for giving us the opportunity to participate in this initiative.

Jon Kraft for his outstanding educational work and the valuable technical assistance provided throughout this project.

Acknowledgements

ANALOG DEVICES

PONTIFICIA UNIVERSIDAD CATOLICA DE CHILE

AC3E
Advanced Center for Electrical and Electronic Engineering

EX UMBRA IN SOLEM
UNIVERSIDAD TECNICA FEDERICO SANTA MARIA

Appendices

2D SLAM: Tree-facing Measurements

Tree at a distance of 3.6 m

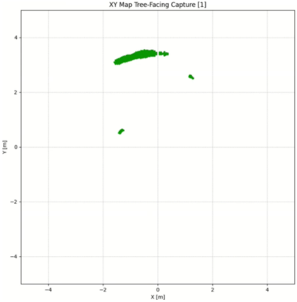

Tree at a distance of 3.0 m

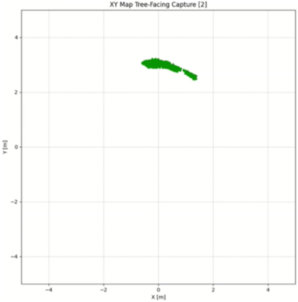

Tree at a distance of 2.4 m

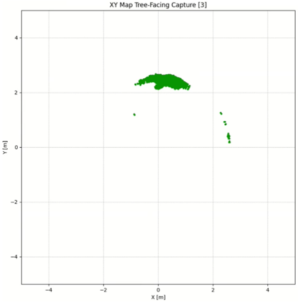

Windowing Effect on Frequency Resolution and Sidelobe Magnitude

Time-domain rect

$$x(t) = \begin{cases} 1, & |t| \le \frac{1}{2} \\ 0, & |t| > \frac{1}{2} \end{cases}$$

Frecuency-domain sinc

$$X(f) = T\,\mathrm{sinc}(fT)$$

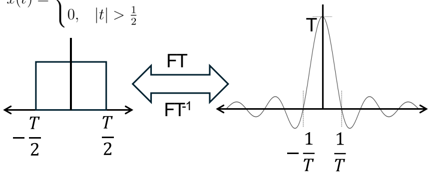

FFT with **rect** window

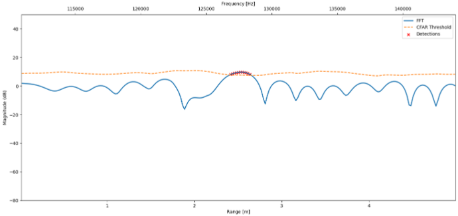

FFT with **Blackman** window

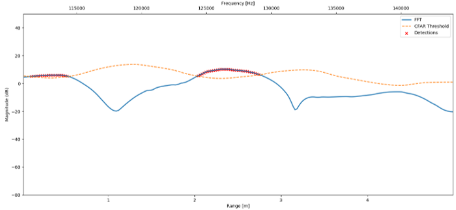

Table 1: Comparison of windows in terms of main lobe and first side lobe.

Window	Main lobe width	Main lobe level (dB)	First side lobe (dB)
Rect	$2/T$	0 dB	−13.3 dB
Hann	$4/T$	−1.5 dB	−31.5 dB
Hamming	$4/T$	−1.8 dB	−42.7 dB
Blackman	$6/T$	−3.9 dB	−58 dB

Magnitude remains similar, but resolution worsens: under identical conditions, Blackman detects 2.0-2.75 m, while Rectangular detects 2.4-2.6 m.

Appendix: Basic notation - Radar and Power Range

P_r	Received power.
P_t	Transmitted power.
G_t, G_r	Transmit and receive antenna gains.
λ	Wavelength.
σ_s	Target radar cross-section.
$r(f_s)$	Target range.
f_b	Beat frequency.
f_{bias}	Frequency bias correction.
c	Speed of light
S	Chirp slope.
B	Bandwidth.
T	Chirp duration
Δr	Range resolution.
r_d	Detection range for a target.
τ	Propagation delay.
f_m	Measured signal frequency.
f_c	Carrier frequency.

Appendix: Basic notation - Linear Frequency Modulation and Averaging

$\phi(t)$	Instantaneous phase of the chirp.
$f(t)$	Instantaneous frequency.
$s_k(t)$	k-th receive chirp signal.
M	Total number of chirps used in the averaging.
$\bar{s}(t)$	Averaged signal over M chirps.

Appendix: Basic notation - Measurements Fusion

$I_{q,m}(\theta_n^s, r(f))$ Intensity matrix.
β Elevation angle.
$\Delta\theta^p, \Delta\theta^s, \Delta\phi^p$ Angular step sizes for PTU pan-tilt and radar steering.
$w_q(\alpha)$ Weight for sweep q based on angular proximity to α.
FOV Radar azimuth field of view.
$\Theta_q(\alpha)$ Relative angle within sweep.
$Q(\alpha)$ Set of sweeps covering azimuth α.
$C(\alpha, \beta, r(f))$ Weighted fusion of intensity across sweeps.

Thank you!

ral.ing.puc.cl

Robotics & Automation Laboratory
School of Engineering
PONTIFICIA UNIVERSIDAD CATÓLICA DE CHILE